From GEO to LEO: First Look Into Starlink In-Flight Connectivity

HyunSeok Daniel Jang
Northwestern University
Evanston, IL, USA
daniel.jang@u.northwestern.edu

Matteo Varvello
Nokia Bell Labs
Murray Hill, NJ, USA
matteo.varvello@nokia.com

Aravindh Raman
Cisco ThousandEyes
London, UK
araram@cisco.com

Yasir Zaki
New York University Abu Dhabi
Abu Dhabi, UAE
yasir.zaki@nyu.edu

Abstract

The growing demand for reliable Internet access during air travel has made in-flight connectivity (IFC) a critical service for commercial airlines. Traditional IFC systems rely on geostationary (GEO) satellites, but their high latency and limited bandwidth hinder user experience. Emerging Low Earth Orbit (LEO) constellations, such as Starlink, promise better network performance. This paper presents the first empirical comparison of IFC performance across GEO and LEO networks, using data from 25 flights operated by 7 airlines. Measurements collected via instrumented Android devices cover key metrics including latency, throughput, and CDN responsiveness. We observe that while GEO systems rely on static and often distant Internet gateways, Starlink clients connect to different gateways that align more closely with flight trajectories, enhancing end-to-end performance through shorter satellite paths. However, DNS-based content filtering on Starlink-equipped flights often affects user geolocation, introducing unnecessary terrestrial delays. Finally, our case study of TCP performance from 2 Starlink flights shows that the BBR congestion control algorithm delivers up to 35× higher throughput than Cubic and Vegas, but with significantly higher retransmissions due to aggressive bandwidth probing.

CCS Concepts

• **Networks** → **Network measurement**; **Network performance analysis**; *Location based services.*

Keywords

In-Flight Connectivity, Satellite Network, Starlink

ACM Reference Format:
HyunSeok, Daniel Jang, Matteo Varvello, Aravindh Raman, and Yasir Zaki. 2025. From GEO to LEO: First Look Into Starlink In-Flight Connectivity. In *Proceedings of the 2025 ACM Internet Measurement Conference (IMC '25), October 28–31, 2025, Madison, WI, USA.* ACM, New York, NY, USA, 11 pages. https://doi.org/10.1145/3730567.3764491

1 Introduction

Commercial airlines have thus far largely relied on geostationary (GEO) satellite networks to provide connectivity to passengers. However, these networks are often affected by high latency and bandwidth constraints due to the large distances involved in signal transmission [17, 30]. In contrast, Low Earth Orbit (LEO) satellite networks, exemplified by Starlink [42], promise significant improvements in latency and overall network performance by leveraging a constellation of satellites closer to Earth.

This paper investigates the performance implications of transitioning from GEO to LEO satellite networks in the context of commercial aviation. Motivated by emerging partnerships between Starlink and major airlines [18, 36], we conducted extensive network diagnostics throughout 25 flights across 7 airlines. Our study employs `AmiGo` [47], an open-source measurement testbed on rooted Android devices to collect a comprehensive set of network performance metrics, including latency, bandwidth, DNS and CDN performance. Notably, while 19 flights operated on GEO networks, the remaining 6 were connected to Starlink's LEO network. In two of these Starlink flights, we use an extended version of `AmiGo` for a closer case study on gateway selection and TCP behavior.

Our research addresses a critical gap in the literature: despite the rapid industry shift towards LEO networks, there is a scarcity of in-depth, real-world performance evaluations contrasting these architectures in the demanding environment of commercial aviation. By presenting novel empirical data, our study aims to illuminate the potential benefits and limitations of LEO networks relative to their GEO counterparts. The key findings of this paper are the following:

Gateway Strategies in IFC. GEO-based IFC providers rely on fixed Internet gateways, often at intercontinental distances from the airplane. In contrast, Starlink clients switch between multiple gateways along each flight path, often much closer to the aircraft (on average 680 km).

Network Performance Comparison. Starlink shows substantial performance advantages over GEO-based IFC, with typical latencies under 40ms (vs GEO's 550+ms) and median downlink bandwidth of 85.2 Mbps (vs GEO's 5.9 Mbps).

DNS Configuration Impact. Starlink employs DNS-based content filtering, often using resolvers distant from the current gateway. This inflates latencies to service providers like Google and Facebook that derive client geolocation via DNS.

BBR's Performance and Tradeoffs in Starlink-Based IFC. In our case study over 2 flights, BBR consistently outperformed Cubic and Vegas in delivery rate, achieving up to 35x higher throughput even across increasing PoP distances. However, its aggressive bandwidth probing led to significantly higher retransmission rates, highlighting a tradeoff between peak performance and network fairness in resource-constrained environments like IFC.

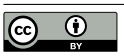

IMC '25, Madison, WI, USA

ACM ISBN 979-8-4007-1860-1/2025/10
https://doi.org/10.1145/3730567.3764491

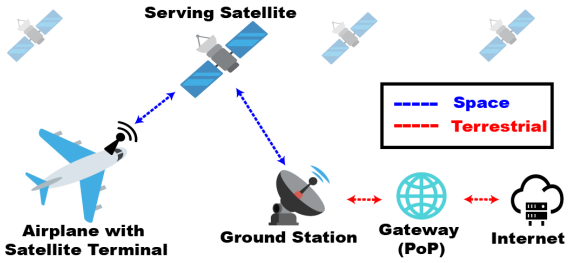

Figure 1: End-to-end IFC client to Internet path.

2 Background and Related Work

Satellite Network Operators (SNOs). SNOs are broadly classified into geostationary (GEO) and Low Earth Orbit (LEO) operators. GEO satellites are positioned approximately 35,786 kilometers (km) above the equator, allowing them to maintain a fixed position relative to the Earth's surface [30]. This fixed orbital location provides consistent coverage over large areas but introduces significant latency due to the long distance that signals must travel. In contrast, LEO SNOs operate at much lower altitudes, typically between 500-2,000 km, which greatly reduces the signal travel time and, consequently, the latency experienced by end users. Yet, this benefit comes at the cost of requiring a large constellation of satellites to ensure continuous global coverage, introducing additional complexities in network management such as frequent handovers and dynamic routing challenges [17].

SNOs for In-Flight Connectivity. Numerous SNOs provide IFC services to commercial airlines today. In the GEO domain, established providers include Inmarsat, ViaSat, SES, and Eutelsat [13, 20, 41, 48]. In the LEO arena, SpaceX's Starlink is rapidly gaining traction by offering lower latency and enhanced performance, thereby challenging the conventional GEO paradigm. Figure 1 visualizes the high-level architecture of satellite-based IFC. The end-to-end data path can be categorized into two segments: *space* and *terrestrial*. The space segment encompasses the radio signal transmission between the user terminal (mounted on aircraft) and ground station (GS). The terrestrial segment comprises the path between the ground station and the Internet backbone. Traffic here is routed through a Point of Presence (PoP), which is the gateway between the satellite and public Internet.

To the best of our knowledge, Rula et al. [39] are the first to shed some light on the performance of IFC systems at the time (2015/2016), examining both direct air-to-ground and mobile satellite service technologies. The study, based on extensive flight measurements, reveals that high latency and packet loss significantly degrade the quality of service for common internet applications. Our work revisits IFC after 8 years with focus on satellite-based services, offering timely insights into how emerging LEO networks (like Starlink) compare to traditional GEO SNOs in addressing the performance challenges previously identified.

Satellite Network Measurements. Existing research on satellite network performance has employed simulations [24, 49], active measurements [22, 23, 29, 31], collaborations with operators [35], and open platforms like M-Lab and RIPE Atlas [32, 37]. Most studies focus on single constellation types (GEO or LEO), with limited cross-constellation comparisons typically using public datasets and stationary user terminals.

Duration	# Flights	SNO	Tool
Dec. 2023 - March 2025	19	GEO	Amigo
March - April 2025	4	LEO	Amigo
April 2025	2	LEO	Amigo & Starlink Extension

Table 1: Number of flights, SNO type, and measurement tool employed at different stages of our data collection campaign.

3 Methodology

Measurement Overview. We build on the `AmiGo` framework [47], an open-source testbed that relies on travelers carrying mobile phones to act as vantage points. `AmiGo` includes a control server for remote management of mobile measurement endpoints (MEs). These MEs are rooted Android devices configured using `termux` [44]. The server exposes RESTful APIs that the MEs use to report their device-level status, such as the current battery level and network connectivity (e.g., WiFi SSID, public IP address).

MEs are automated to periodically run shell scripts that collect various network metrics in the background. We provide a detailed breakdown of these measurements in Appendix Table 5. Speedtest [33] measures download/upload throughput and latency, utilizing (by default) one of Ookla's servers with the minimum Round-Trip Time (RTT) from the client's IP geolocation as the endpoint [34]. ME further runs traceroutes to major content providers (Google, Facebook) and DNS resolvers (Cloudflare DNS, Google DNS) via `mtr` [27]. We also identify the current DNS resolver by querying NextDNS [4] (see Section 4.2). Finally, we download a popular JavaScript library (jquery.min.js) from five CDN providers with a global footprint: Google CDN, Cloudflare, Microsoft Ajax, jsDelivr, and jQuery. For this test, we use curl [45] formatted to report the DNS lookup time and the total download time, while also collecting HTTP headers to identify cache-related information (more on Section 4.3).

To determine which SNO the ME is connected to during a flight, we use its public IP address and infer the associated Autonomous System Number (ASN) from WHOIS database and ipinfo [21]. In cases of a Starlink connection (AS14593), we identify the specific Point of Presenece (PoP) in use through a reverse DNS lookup, which maps the public IP address with a hostname in the form of `customer.LOCATION.pop.starlinkisp.net`.

Starlink Extension. We extend `AmiGo` to analyze the performance differences between Starlink's various PoPs and their impact on network latency. In consumer Starlink terminals, the gRPC interface typically provides network diagnostics including real-time latency measurements to the gateway [43, 50]. However, gRPC queries were not permitted during our measurement flights.

We instead deploy cloud servers in multiple AWS regions strategically located along the flight path. This allows MEs to conduct high-frequency (10 ms granularity) UDP ping measurements via IRTT [19] to the *closest* AWS server, *i.e.,* co-located to the current PoP used. Each measurement session runs for 5 minutes, providing

SNO	ASN	Airline	PoPs(s)
Inmarsat	AS31515	Qatar Airways	Staines (UK) Greenwich (US)
Intelsat	AS22351	KLM Airlines Air France	Wardensville (US)
Panasonic	AS64294	Etihad Airways Air France	Lake Forest (US)
SITA	AS206433	Etihad Airways Qatar Airways	Amsterdam (NL)
		Emirates Saudia	Lelystad (NL)
ViaSat	AS40306	JetBlue Airways	Englewood (US)
Starlink	AS14593	Qatar Airways	*Table 7 in Appendix*

Table 2: Satellite Network Operators measured.

time-series data for fine-grained comparison of latency characteristics across PoPs.

We further piggyback on these AWS servers to evaluate TCP performance. Specifically, we perform file transfers under different TCP congestion control algorithms (CCAs), configured with `sysctl` [25] at the AWS server. We rely on a *receiver* which runs in the ME and opens a connection towards a server. The *sender* runs in AWS and accepts connections and transfer test files of a desired size (1.8 GB, by default). During each file transfer, fine-grained socket statistics are collected at the server via `ss` [26]. ME automatically runs the two tests sequentially when it connects to a new PoP.

We retrieve fine-grained aircraft position data from an online flight-tracking service [14]. Since each commercial flight has a unique ID that generally follows a consistent route, we estimate its path using previous route data. These projected paths allow us to identify anticipated Starlink PoPs and corresponding AWS regions for the two aforementioned measurements. We also use the position data to correlate network performance with aircraft location.

Data Collection. As summarized in Table 1, we launched a measurement campaign from December 2023 to April 2025, recruiting 10 volunteers who traveled on commercial airplanes equipped with in-flight WiFi. Each volunteer carried an `AmiGo` ME (Samsung Galaxy A34 5G [16]) to run network measurements during the flight. Volunteers were instructed to carry these devices and refrain from using them to avoid interference with the measurements.

Our dataset comprises 19 flights with GEO SNOs recorded between December 2023 and March 2025, spanning 7 airlines operating across 22 airports in 15 countries. Details of these flights, including their respective test counts, are summarized in the Appendix (see Table 6). In addition, we began our investigation of Starlink Aviation in March 2025, following its initial deployment on Qatar Airways in November 2024 [36]. This portion of our dataset includes 6 Qatar Airways flights: 2 DOH-JFK, 2 JFK-DOH, 1 DOH-LHR, and 1 LHR-DOH route (see Appendix Table 7 for a breakdown of tests conducted). Note that Starlink Aviation remains in the early adoption phase, available only on limited flight paths and airplane models. For Qatar Airways, the service is scheduled to be available on just 40 Boeing 777s (17% of their fleet) serving 28 airports by June 2025 (15% of their 181 international destinations) [7, 8, 12]

We utilized the Starlink extension of `AmiGo` only for the final two flights between Doha and London, after discovering that the operator's gRPC interface was inaccessible during the earlier flights.

Figure 2: Flight path and PoP locations during Doha-Madrid route, November 2024. The aircraft utilized Inmarsat (AS31515).

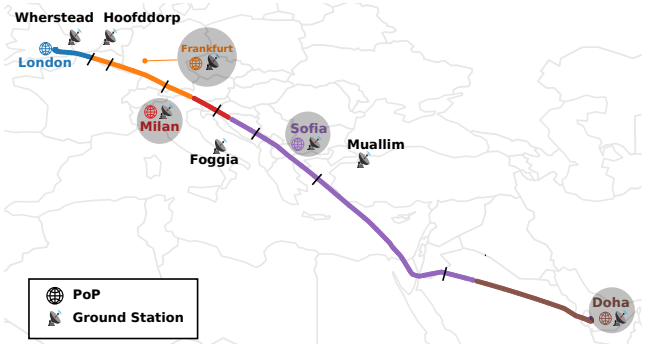

Figure 3: Doha–London flight path (Apr 2025) color-coded by Starlink PoP. Segments closest to each ground station (GS) are marked by black vertical lines. Grey circles indicate cities where PoP and GS are co-located.

We instrumented AWS EC2 t3.xlarge instances [10] close to intercepted PoPs: London (eu-west-2), Milan (eu-south-1), Frankfurt (eu-central-1), and UAE (me-central-1)—, reflecting connections to Starlink PoPs in London, Milan, Frankfurt, Sofia, Warsaw, and Doha observed in our dataset. There is currently no AWS region in reasonable proximity to Sofia and Warsaw. Our collected dataset is publicly available at [11].

4 Starlink vs GEO

4.1 Tomography of Public Gateways

For GEO clients, we find that only one or two PoPs are used per flight, thus often geographically distant from the aircraft's position. Table 2 summarizes the PoP locations observed across all GEO-based flights in our dataset. Figure 2 maps this behavior during a Qatar Airways flight from Doha to Madrid in November 2024, where the client connected via Inmarsat (AS31515, GEO). Throughout the 7-hour journey, all traffic was routed through two PoPs located in Staines (UK), and Greenwich (US), approximately 7,380 km away from the flight path at its furthest point.

In contrast, we observe that PoP locations for Starlink clients change dynamically based on the aircraft position. Figure 3 shows an example with a Qatar Airways flight from Doha to London in April 2025, where the client's traffic was routed through five Starlink PoPs. The flight's trajectory is color-coded to indicate which PoP was used during each segment of the journey. The map shows that PoPs were utilized for significantly varying time periods. The Sofia PoP maintained the longest connection, serving approximately 3 hours and covering over 2,700 kilometers of the flight path, while the Milan PoP provided connectivity for only about 22 minutes, covering just 330 kilometers. PoP transitions did not always follow simple geographic proximity rules. For instance, the connection switched from Doha to Sofia despite Doha remaining closer to the

PoP	Google	FB	jsDelivr (Fastly)	jsDelivr (Cloudf.)	jQuery	Cloudf.
Doha	LDN AMS	LDN MRS	LDN	DOH	MRS	DOH SIN
Sofia	LDN AMS FRA	LDN PAR MRS	LDN	SOF	SOF	SOF
Milan	LDN AMS FRA	LDN PAR	LDN		MXP SOF MAD FRA	MXP SOF MAD
Frankfurt	LDN AMS	LDN PAR	LDN	FRA	FRA	FRA
Madrid	LDN FRA	LDN	LDN	MAD	MAD	MAD
London	LDN AMS	LDN	LDN	LDN	LDN	LDN
NY	NYC	NYC	NYC	NYC	NYC	NYC

Table 3: Cache location per provider and Starlink PoP, inferred from airport codes in traceroute (Google, Facebook) and HTTP headers (jQuery, jsDelivr, Cloudflare).

aircraft at the transition point. We observed these patterns across all 6 Starlink flights in our dataset, with their details of PoP usage provided in the Appendix (Table 7).

To provide a potential explanation of the previous behavior, Figure 3 also maps the locations of Starlink's ground stations (GS) obtained from crowd-sourced datasets [15, 40]. By identifying the geographically closest GS along the flight path, we conjecture that PoP selection could be determined by GS availability rather than direct aircraft-to-PoP proximity. As a hypothetical example, when the plane was within range of the Doha GS, it was assigned to the Doha PoP. Later, as the flight progressed, the clients switched to Sofia PoP when the Muallim (Turkey) GS became the nearest.

4.2 DNS Configuration

In-flight connectivity providers commonly employ DNS filtering to restrict access to bandwidth-intensive or blacklisted domains. We used NextDNS [4] to identify the DNS resolvers used throughout the flights. NextDNS operates as an authoritative DNS service for custom domains with a time-to-live (TTL) of zero, ensuring that resolvers always query it – granted that TTL is respected. It then echoes back to its users the unicast address of the resolver that made the request. This allows us to geolocate the resolver's IP address even when anycast is used between client and resolver.

We detail DNS resolvers and locations for GEO SNOs in the Appendix (see Table 4). We identified 7 unique DNS hosts across the GEO SNOs, with ViaSat and SITA employing their own DNS servers. Most DNS resolvers were located within the same country as the client's PoP, except for Inmarsat which temporarily used Packet Clearing House (Amsterdam) despite its current PoP being in Staines (England).

Conversely, all the Starlink-based flights in our dataset used CleanBrowsing [1], a popular DNS filtering technology for safe browsing. CleanBrowsing uses anycast to direct users to the nearest DNS resolver, ideally located near the PoP used by Starlink at a given time (see Figure 3, for example). However, with only 50 anycast locations globally [2], CleanBrowsing often introduces considerable path inflation between PoP and DNS resolver. For example, during

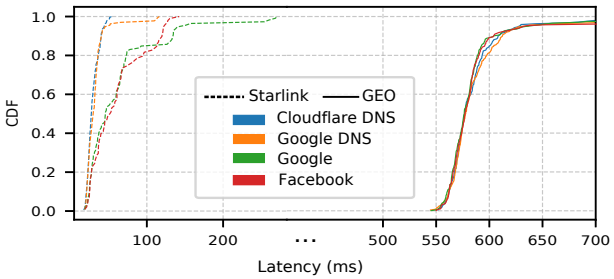

Figure 4: Latency CDF per provider (Starlink vs GEO).

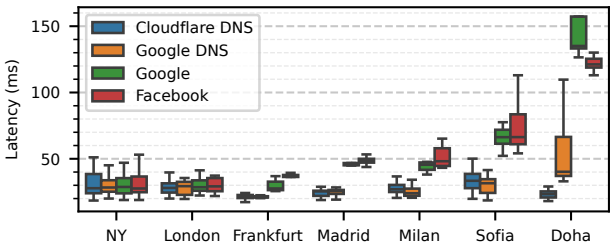

Figure 5: Latency to service providers per Starlink PoP.

flights over Europe, DNS queries are mostly resolved via London, even when using the Sofia PoP, located 1,700 km away.

4.3 Network Performance

Latency. Using traceroute data, Figure 4 compares latency of GEO-based IFC and Starlink to four global service providers: two DNS services (Cloudflare, Google DNS) and two content providers (Google, Facebook). GEO SNOs consistently show latencies about an order of magnitude longer, with over 99% of 949 tests exceeding 550 ms. In contrast, Starlink shows much lower delays (Mann–Whitney U[1], $p < 0.001$ for all provider comparisons): 90% of 322 DNS traceroutes resolve within 40 ms, while 84.8% of 112 to Google and 81.6% of 80 tests to Facebook are under 100 ms.

For Starlink, Figure 4 shows significantly higher latencies to Google and Facebook compared to Cloudflare and Google DNS ($p < 0.001$). Given all these providers have global infrastructures, we would normally expect similar latency performance. However, a key distinction lies in how traceroute is executed. For Google and Cloudflare DNS, traceroute targets (anycast) IP addresses (8.8.8.8 and 1.1.1.1), thus bypassing DNS resolution. In contrast, traceroutes to Google and Facebook begin with a DNS lookup, which returns an IP address based on the geolocation of the DNS resolver in use. Starlink usage of CleanBrowsing introduces a geolocation mismatch, e.g., redirecting traffic to London despite being connected to Doha (see Table 3), causing inefficiencies in the terrestrial path.

We show that such DNS configuration introduced additional delay in Figure 5, which breaks down the Starlink latency results from Figure 4 by PoP. For New York and London PoPs, latency across all providers is consistently low, averaging approximately 29 ms. For the remaining PoPs, latencies to Google and Facebook were inflated due to CleanBrowsing DNS geolocation inefficiencies. This latency inflation largely increases with distance from the resolver's

[1]Unless otherwise noted, all pairwise comparisons of latency and throughput distributions were evaluated using the Mann–Whitney U test

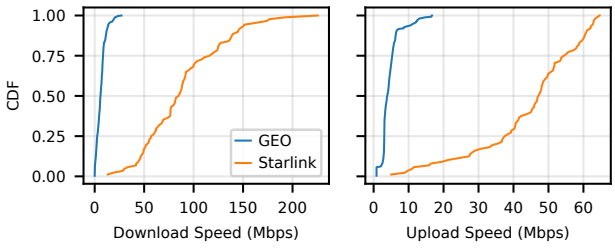

Figure 6: Downlink (left) and uplink (right) bandwidth: Starlink vs. GEO (Ookla speedtests).

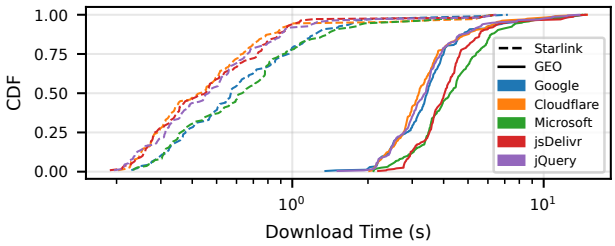

Figure 7: CDF of download time for jQuery library across CDNs, with results from Starlink and GEO SNOs shown in dashed lines and solid lines, respectively.

geolocation, resulting in 1.2× (Frankfurt) to 4.6× (Doha) higher delays compared to those observed in NY and London PoPs.

Bandwidth. We use Ookla speedtests [33] to measure IFC bandwidth. Figure 6 compares download and upload CDFs between 88 tests with Starlink and 264 tests with GEO SNOs. Similar to latency results, Starlink consistently achieves higher bandwidth. For download, Starlink showed a median of 85.2 Mbps with an IQR of 60.2 Mbps, significantly outperforming GEO SNOs (median 5.9 Mbps, IQR 5.7 Mbps; $p < 0.001$). Notably, 83% of tests with GEO SNOs recorded download speeds below 10 Mbps, less than Starlink's minimum observed downlink at 18.6 Mbps. The performance gap is similarly substantial for uplink, where Starlink reported a median of 46.6 Mbps (IQR 17.8 Mbps) versus 3.9 Mbps (IQR 2.2 Mbps) for GEO SNOs ($p < 0.001$).

To explore how the choice of SNO impacts application-layer performance and content delivery for IFC, we measure the download time for `jquery.min.js` (a popular JavaScript library [46]) from five global CDN providers. Figure 7 presents the CDF of download times, comparing results from 1,184 tests with GEO SNOs (solid lines) and 547 tests with Starlink (dashed lines). For GEO SNOs, the fastest download time was recorded at 1.35 seconds, with 96.7% of tests requiring 2-10 seconds. In contrast, Starlink demonstrated dramatically better performance across all CDN providers ($p < 0.001$), with over 87% of download tests completing in under one second. The intersection of the two CDF tails in the figure shows that ~7% of the slowest Starlink downloads lasted longer than the fastest GEO downloads for each CDN. These Starlink outliers suffered from long DNS resolution times, which accounted for 74% of the total download duration, on average; this is likely a result of DNS cache misses requiring recursive resolution via authoritative nameservers.

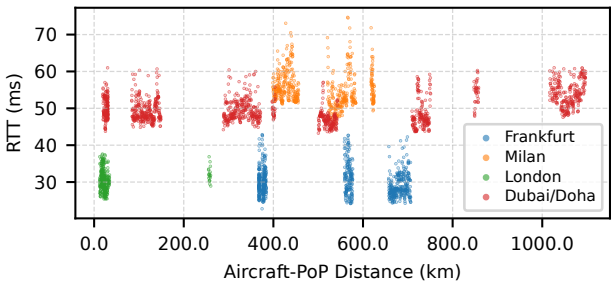

Figure 8: Latency (to closest AWS server) as a function of airplane's distance to Starlink PoP in use.

Finally, we analyze the impact of DNS-based geolocation errors on CDN providers accessed from Starlink IFC. Table 3 summarizes cache node locations inferred from geographic identifiers in HTTP headers (e.g., `x-served-by` from Fastly, `cf-ray` from Cloudflare) [3, 6]. We examined jQuery (Fastly), jsDelivr (Fastly and Cloudflare), and direct Cloudflare tests. Requests via Cloudflare, both direct and through jsDelivr, were routed to caches near the Starlink PoP, thanks to BGP anycast-based routing that bypasses DNS-based geolocation errors. Similar cache selection is achieved by jQuery, using Fastly's anycast. In contrast, jsDelivr requests served by Fastly were routed to London, regardless of PoP, suggesting DNS-based cache selection. This routing mismatch impacted performance: jsDelivr over Cloudflare ($n = 51$) was 34.7% faster on average than over Fastly ($n = 58$; $p < 0.001$).

5 A Closer Look at Starlink

In this section, we present a case study from 2 Qatar Airways flights on the Doha-London route, where we employed AWS endpoints to conduct high-frequency UDP `ping` as well as TCP file transfers. We first examine the latency impact of Starlink dynamic gateway selection, followed by implications of TCP CCA.

5.1 Location-Based Delay

We define *plane-to-PoP* distance as the haversine distance between the plane's ground projection and the PoP in use. Figure 8 shows RTT to the geographically closest AWS server to each PoP (filtered outliers below 95th percentile) as a function of plane-to-PoP distance. Each colored cluster represents a set of high-frequency pings (IRTT) conducted while connected to the PoP indicated by the color, e.g., red for Doha approximated by the closest AWS server (Dubai).

The Doha PoP (red) has the most number of tests since it was utilized longer than other PoPs (see Figure 3). Note that while the Sofia PoP was used even longer, no AWS server is available in the region, so no IRTT measurement was run for this PoP. The figure shows that Milan (orange) and Doha (red) PoPs exhibit significantly higher latency (medians 54.3 ms and 49.1 ms) compared to London (green) and Frankfurt (blue) PoPs (medians 30.5 ms and 29.5 ms). These latency differences persisted regardless of plane-to-PoP distance. Further latency measurements to Starlink PoPs (traceroute hops with address 100.64.0.1) reveal no statistically significant correlation with distance below 800 km ($p > 0.05$), suggesting that observed differences are not attributable to the bent-pipe *space* segment in the end-to-end path.

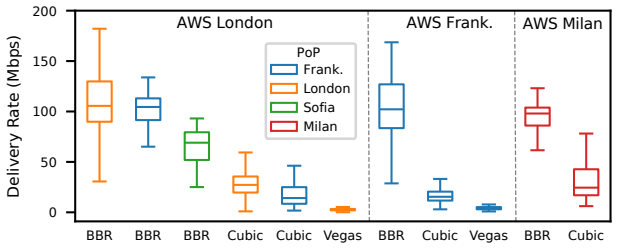

Figure 9: Delivery rate (goodput) from AWS servers to clients using different Starlink PoPs and TCP CCAs.

To further explain the previous result, we examine differences in peering arrangements. Milan and Doha PoPs route traffic through intermediaries (AS57463 and AS8781) which induces additional latency. In contrast, London and Frankfurt PoPs establish direct peering relationships with major service providers, eliminating these intermediary hops. We cross-validated these findings using data from Ripe Atlas [38], analyzing traceroutes to Facebook and Google conducted from probes using the same Frankfurt, London, and Milan Starlink PoPs (no probe using the Doha PoP was available) from March 1st to April 20th, 2025. Out of 9,598 traceroutes originating from the Milan POP, 95.4% included traversals to transit providers. This stood in stark contrast to Frankfurt and London PoPs, which exhibited such patterns in only 0.09% of 9,583 and 1.7% of 9,596 traceroutes, respectively.

5.2 TCP Performance

We here analyze TCP performance from file transfer tests, where different AWS servers were selected as endpoints based on the Starlink PoP in use. We evaluate three popular CCAs: BBR, Cubic, and Vegas. We prioritized using the closest available server to each PoP, but also included London for Frankfurt and Sofia to assess distance effects on CCA performance. Certain PoPs could not test all CCAs due to constraints: Sofia lacks a nearby AWS region, and Milan's short connection window prevented Vegas tests (Appendix Table 8 summarizes the experimental setups).

Figure 9 plots the delivery rates (goodput) obtained across all tests, organized by AWS server location and color-coded by PoP. For tests when server and PoP were geographically aligned (ex: London-London), BBR consistently outperforms other CCAs, achieving median delivery rates of 98-105 Mbps, roughly 3-6x higher than Cubic and 24-35x higher than Vegas. The figure also shows that BBR's performance gradually degrades as PoP distance increases. Comparing results in London AWS accessed through London, Frankfurt, and Sofia PoPs, the median (IQR) delivery rate drops from 105.5 (40) Mbps to 104.5 (21) Mbps to 69 (27) Mbps, respectively. However, BBR remains superior to what Cubic (15.4-27.2 Mbps) and Vegas (<5 Mbps) achieve even in geographically aligned conditions. While such goodput discrepancies can be attributed to BBR's aggressive window management strategy, we also observed its potential tradeoff in substantially higher retransmission rates (see Appendix Section A.7). These characteristics raise network fairness concerns in resource-constrained environments like IFC, where BBR flows might monopolize limited satellite bandwidth.

6 Discussion

Data Representativeness While this study provides a preliminary comparison of IFC performance between GEO satellite network operators and Starlink, the findings should be interpreted within the context of several limitations. Our dataset, comprising 25 flights, is modest in scale and does not fully absorb the potential impact of flight-specific variables, such as the number of passengers and their generated traffic, or weather-related factors (e.g., heavy rain or turbulence). We also acknowledge the limited geographic coverage, which spanned only 23 airports across 15 countries, with flight paths largely concentrated in the Middle East and Europe. Furthermore, there is a temporal gap in our data collection, with the majority of GEO connectivity measurements taken from late 2023 to 2024, while all LEO connectivity data was collected from February to April, 2025. This discrepancy may not capture subsequent temporal changes or service enhancements within the GEO satellite networks.

Future Work Building on the limitations of this study, future research could expand measurements to cover a broader range of airlines and SNOs, such as Amazon's Project Kuiper, which recently partnered with JetBlue Airways [9]. Geographic scope is critical as well. For instance, anecdotal reports suggest Starlink connectivity is unavailable over Indian and Chinese airspace [5]. Starlink performance can also vary with latitude, as higher latitudes may increase the distance to satellite constellations and network latency. Incorporating such regional constraints into a broader dataset would allow for more accurate characterization of service availability and performance worldwide. Futhermore, our measurement scope was bounded by network metrics collected by the `Amigo` testbed. Consequently, we were unable to study the performance of common passenger applications or their quality of experience (QoE), such as video streaming or real-time voice communication. Extending future measurement frameworks to include application-level metrics would enable a more direct evaluation of IFC user experience.

Beyond expanding the dataset, several specific research avenues warrant exploration. A valuable comparative analysis would be to measure the performance of GEO and LEO satellite links in both stationary and in-flight settings, which could help isolate the performance impacts attributable specifically to mobility. Finally, given the logistical challenges with conducting large-scale active measurements on commercial aircraft, future work could explore novel methodologies to characterize traffic or map IP address ranges associated with IFC from passive measurements.

7 Conclusion

We present the first in-situ characterization of Starlink Aviation, comparing its performance with GEO-based in-flight connectivity (IFC) across 25 flights operated by 7 airlines. Unlike GEO providers that rely on fixed PoPs, Starlink clients were routed through multiple PoPs during flights, shortening the satellite bent-pipe link. Consequently, we find that variations in end-to-end latency largely stem from terrestrial factors, particularly peering relationships and geolocation inefficiencies due to DNS-based content filtering, rather than from plane-PoP proximity. Finally, our preliminary dataset shows that BBR achieves higher goodput than Cubic and Vegas, but with increased retransmissions. These results highlight both the promise and current limitations of LEO satellite networks for IFC.

References

[1] 2025. *CleanBrowsing | DNS Filtering Platform.* https://cleanbrowsing.org/ Accessed: 2025-05-04.

[2] 2025. CleanBrowsing Network Status. https://cleanbrowsing.org/status/

[3] 2025. Cloudflare HTTP headers. https://developers.cloudflare.com/fundamentals/reference/http-headers/

[4] 2025. NextDNS. https://nextdns.io/

[5] 2025. Starlink on a Commercial Airline. https://www.reddit.com/r/Starlink/comments/1l9dpim/starlink_on_a_commercial_airline/.

[6] 2025. X-Served-By | Fastly Documentation. https://www.fastly.com/documentation/reference/http/http-headers/X-Served-By/

[7] Qatar Airways. 2025. Fleet Qatar Airways. https://www.qatarairways.com/en/fleet.html

[8] Qatar Airways. 2025. Starlink. The fastest on-board Wi-Fi in the sky | Qatar Airways. https://www.qatarairways.com/en-ae/onboard/connectivity.html

[9] Amazon Staff. 2025. JetBlue chooses Amazon's Project Kuiper for faster, free in-flight Wi-Fi. https://www.aboutamazon.com/news/innovation-at-amazon/jetblue-amazon-project-kuiper-in-flight-wifi-partnership.

[10] Amazon Web Services. 2025. *Amazon EC2 T3 Instances.* Amazon Web Services. https://aws.amazon.com/ec2/instance-types/t3/ Accessed: 2025-05-06.

[11] comnetsAD. 2025. From GEO to LEO IMC2025. https://github.com/comnetsAD/From_GEO_to_LEO_IMC2025.

[12] Flight Connections. 2025. Qatar Airways Flights and Destinations - FlightConnections. https://www.flightconnections.com/route-map-qatar-airways-qr

[13] Eutelsat. 2021. *Aviation Inflight Connectivity.* https://www.eutelsat.com/en/satellite-communication-services/aviation-inflight-connectivity.html

[14] Flightradar24 AB. 2025. *Flightradar24.* https://www.flightradar24.com/ Accessed April 28, 2025.

[15] Google My Maps user. 2025. Unofficial Starlink Global Gateways & PoPs. https://www.google.com/maps/d/u/0/viewer?mid=1805q6rlePY4WZd8QMOaNe2BqAgFkYBY&hl=en_US&ll=29.92773521630133%2C35.02090615416515&z=4 Accessed April 29, 2025.

[16] GSMArena. 2023. *Samsung Galaxy A34 - Full phone specifications.* GSMArena.com. https://www.gsmarena.com/samsung_galaxy_a34-12074.php

[17] Mark Handley. 2018. Delay is Not an Option: Low Latency Routing in Space. In *Proceedings of the 17th ACM Workshop on Hot Topics in Networks* (Redmond, WA, USA) *(HotNets '18)*. Association for Computing Machinery, New York, NY, USA, 85–91. https://doi.org/10.1145/3286062.3286075

[18] Hawaiian Airlines. 2025. Hawaiian Airlines Now Offering Fast and Free Starlink Wi-Fi Across Entire Airbus Fleet. https://newsroom.hawaiianairlines.com/releases/hawaiian-airlines-now-offering-fast-and-free-starlink-wi-fi-across-entire-airbus-fleet Accessed: 2025-03-13.

[19] Paul Heist. 2025. Isochronous Round-Trip Tester (IRTT). https://github.com/heistp/irtt. Accessed: 2025-04-22.

[20] Inmarsat. 2023. *Inmarsat plans fastest inflight broadband for business aviation.* https://www.inmarsat.com/en/news/latest-news/aviation/2023/fastest-inflight-broadband-plans-for-business-aviation.html

[21] Ipinfo. 2025. The trusted source for IP address data. https://ipinfo.io/developers

[22] Liz Izhikevich, Manda Tran, Katherine Izhikevich, Gautam Akiwate, and Zakir Durumeric. 2024. Democratizing LEO Satellite Network Measurement. *Proc. ACM Meas. Anal. Comput. Syst.* 8, 1, Article 13 (Feb. 2024), 26 pages. https://doi.org/10.1145/3639039

[23] Mohamed M. Kassem, Aravindh Raman, Diego Perino, and Nishanth Sastry. 2022. A Browser-side View of Starlink Connectivity. In *Proceedings of the 22nd ACM Internet Measurement Conference (IMC'22)*. Nice, France.

[24] Simon Kassing, Debopam Bhattacherjee, André Baptista Águas, Jens Eirik Saethre, and Ankit Singla. 2020. Exploring the "Internet from space" with Hypatia. In *Proceedings of the ACM Internet Measurement Conference* (Virtual Event, USA) *(IMC '20)*. Association for Computing Machinery, New York, NY, USA, 214–229. https://doi.org/10.1145/3419394.3423635

[25] Michael Kerrisk. [n. d.]. *sysctl(8) - Linux manual page.* Linux man-pages project. https://man7.org/linux/man-pages/man8/sysctl.8.html Accessed: April 30, 2025.

[26] Michael Kerrisk et al. 2025. *ss(8) - Linux manual page.* https://man7.org/linux/man-pages/man8/ss.8.html Accessed April 28, 2025.

[27] Matt Kimball. 2025. My traceroute (mtr). https://www.bitwizard.nl/mtr/

[28] Zeqi Lai, Zonglun Li, Qian Wu, Hewu Li, Weisen Liu, Yijie Liu, Xin Xie, Yuanjie Li, and Jun Liu. 2024. Mind the Misleading Effects of LEO Mobility on End-to-End Congestion Control. In *Proceedings of the 23rd ACM Workshop on Hot Topics in Networks* (Irvine, CA, USA) *(HotNets '24)*. Association for Computing Machinery, New York, NY, USA, 34–42. https://doi.org/10.1145/3696348.3696867

[29] Sami Ma, Yi Ching Chou, Haoyuan Zhao, Long Chen, Xiaoqiang Ma, and Jiangchuan Liu. 2023. Network Characteristics of LEO Satellite Constellations: A Starlink-Based Measurement from End Users. In *IEEE INFOCOM 2023 - IEEE Conference on Computer Communications*. 1–10. https://doi.org/10.1109/INFOCOM53939.2023.10228912

[30] Gérard Maral, Michel Bousquet, and Zhili Sun. 2020. *Satellite Communications Systems: Systems, Techniques and Technology* (6th ed.). Wiley.

[31] François Michel, Martino Trevisan, Danilo Giordano, and Olivier Bonaventure. 2022. A first look at starlink performance. In *Proceedings of the 22nd ACM Internet Measurement Conference*. 130–136.

[32] Nitinder Mohan, Andrew E. Ferguson, Hendrik Cech, Rohan Bose, Prakita Rayyan Renatin, Mahesh K. Marina, and Jörg Ott. 2024. A Multifaceted Look at Starlink Performance. In *Proceedings of the ACM Web Conference 2024* (Singapore, Singapore) *(WWW '24)*. Association for Computing Machinery, New York, NY, USA, 2723–2734. https://doi.org/10.1145/3589334.3645328

[33] OOKLA. 2024. Speedtest CLI, Internet connection measurement for developers. https://www.speedtest.net/apps/cli.

[34] Carin Overturf. 2019. How does Speedtest know where I am? https://help.speedtest.net/hc/en-us/articles/360039162893-How-does-Speedtest-know-where-I-am

[35] Daniel Perdices, Gianluca Perna, Martino Trevisan, Danilo Giordano, and Marco Mellia. 2022. When satellite is all you have: watching the internet from 550 ms. In *Proceedings of the 22nd ACM Internet Measurement Conference* (Nice, France) *(IMC '22)*. Association for Computing Machinery, New York, NY, USA, 137–150. https://doi.org/10.1145/3517745.3561432

[36] Qatar Airways. 2025. Qatar Airways Equips 30th Boeing 777 with Starlink, Outpacing Original Timeline by 70 Per Cent. https://www.qatarairways.com/press-releases/en-WW/247298-qatar-airways-equips-30th-boeing-777-with-starlink-outpacing-original-timeline-by-70-per-cent Accessed: 2025-03-13.

[37] Aravindh Raman, Matteo Varvello, Hyunseok Chang, Nishanth Sastry, and Yasir Zaki. 2023. Dissecting the Performance of Satellite Network Operators. In *Proceedings of the 19th International Conference on emerging Networking EXperiments and Technologies (CoNEXT'23)*. Paris, France.

[38] RIPE NCC. 2025. RIPE Atlas. https://atlas.ripe.net/. Accessed: 2025-04-27.

[39] John P. Rula, James Newman, Fabián E. Bustamante, Arash Molavi Kakhki, and David Choffnes. 2018. Mile High WiFi: A First Look At In-Flight Internet Connectivity. In *Proceedings of the 2018 World Wide Web Conference* (Lyon, France) *(WWW '18)*. International World Wide Web Conferences Steering Committee, Republic and Canton of Geneva, CHE, 1449–1458. https://doi.org/10.1145/3178876.3186057

[40] satellitemap.space. 2025. *Live Starlink Satellite and Coverage Map.* https://satellitemap.space/ Accessed April 29, 2025.

[41] SES. 2024. *SES Launches SES Open Orbits™ Inflight Connectivity Network.* https://www.ses.com/press-release/ses-launches-ses-open-orbitstm-inflight-connectivity-network

[42] Starlink. 2025. Starlink Aviation - High-Speed, Low-Latency Inflight Internet. https://www.starlink.com/business/aviation Accessed: 2025-03-13.

[43] Hammas Bin Tanveer, Mike Puchol, Rachee Singh, Antonio Bianchi, and Rishab Nithyanand. 2023. Making Sense of Constellations: Methodologies for Understanding Starlink's Scheduling Algorithms. In *Companion of the 19th International Conference on Emerging Networking EXperiments and Technologies* (Paris, France) *(CoNEXT 2023)*. Association for Computing Machinery, New York, NY, USA, 37–43. https://doi.org/10.1145/3624354.3630586

[44] termux. 2025. Android terminal emulator and Linux environment app. https://termux.com/.

[45] The curl Project. 2025. curl man page. https://curl.se/docs/manpage.html. curl version 8.16.1.

[46] The jQuery Foundation. 2025. jQuery: The Write Less, Do More, JavaScript Library. https://jquery.com/ Accessed: 2025-05-15.

[47] Matteo Varvello and Yasir Zaki. 2023. A Worldwide Look Into Mobile Access Networks Through the Eyes of AmiGos. In *2023 7th Network Traffic Measurement and Analysis Conference (TMA)*. 1–10. https://doi.org/10.23919/TMA58422.2023.10198920

[48] Viasat. 2024. *In-Flight Connectivity for Commercial Aviation.* https://www.viasat.com/aviation/commercial-aviation/in-flight-connectivity/

[49] Junyong Wei, Suzhi Cao, Siyan Pan, Jiarong Han, Lei Yan, and Lei Zhang. 2020. SatEdgeSim: A Toolkit for Modeling and Simulation of Performance Evaluation in Satellite Edge Computing Environments. In *2020 12th International Conference on Communication Software and Networks (ICCSN)*. 307–313. https://doi.org/10.1109/ICCSN49894.2020.9139057

[50] Jinwei Zhao and Jianping Pan. 2024. LENS: A LEO Satellite Network Measurement Dataset. In *Proceedings of the 15th ACM Multimedia Systems Conference* (Bari, Italy) *(MMSys '24)*. Association for Computing Machinery, New York, NY, USA, 278–284. https://doi.org/10.1145/3625468.3652170

A Appendix

A.1 Ethics

The goal of this study is to evaluate in-flight connectivity performance across multiple airlines and technologies, specifically comparing GEO and LEO satellite providers. Study participants were asked to carry our provisioned mobile devices throughout their

flights, keep them charged, and, when available, connect them to the onboard Wi-Fi. They were explicitly instructed not to install personal applications, log into any accounts, or store personal data on these devices. Consequently, no personal or sensitive information was recorded at any point during the study. Furthermore, to minimize potential impact on other passengers in flight, we carefully limited the frequency and data volume of network diagnostics conducted by our devices, and no interference with service quality was reported during or after the flights.

To ensure ethical compliance, we obtained Institutional Review Board (IRB) approval (anonymized to preserve the double-blind protocol) and two authors completed CITI research-ethics training. All participants reviewed and signed an informed-consent document, with ample opportunity to ask questions about the data being collected.

A.2 Measurement Overview

Table 5 presents a breakdown of network diagnostic and tests available across the Amigo testbed and its Starlink Extension. We provide a detailed description, the type of visibility (e.g., latency, bandwidth), and the frequency of execution for each test. Note that while the tests were configured to run at the listed intervals, they only executed when sufficient internet connectivity was available. Standard tests like device status reports, speed tests, traceroutes, DNS lookups, and CDN performance tests run at regular intervals for both Amigo and Amigo with Starlink Extension. High-frequency UDP pings and TCP file transfers are exclusive to the Starlink Extension.

A.3 GEO-based Flights

From December 2023 and March 2025, we conducted network measurements in 19 flights with GEO satellite connectivity. For each of these flights, Table 6 details the origin and destination airports (as IATA codes), departure date, the SNO and its ASN providing connectivity, PoP location(s), and the number of each tests succesfully conducted.

A.4 DNS Configuration for GEO SNOs

Table 4 summarizes the DNS configurations used by different GEO SNOs in our dataset. For each SNO, we identify the DNS hosting provider with the corresponding ASN and the resolver's geolocation. We obseve that some SNOs operate their own DNS infrastructure (e.g., SITA, ViaSat) while others leverage third-party providers like Cloudflare or Google. Temporal changes in DNS configuration are also noted for Panasonic, which switched providers between our measurement periods.

A.5 Starlink Flights

Table 7 provides an overview of the 6 Qatar Airways flights with Starlink connectivity in our dataset. For each flight, we identify the Starlink Points of Presence (PoPs) detected by our measurement endpoints and their respective connection durations in minutes. These durations represent connection periods to our `AmiGo` server only, calculated as the interval between first and last IP reports, excluding any periods when the measurement device was inactive

SNO	DNS Host	DNS Location
Inmarsat (AS31515)	Cloudflare (AS1335) Packet Clearing House (AS42)	NL, US
Intelsat (AS22351)	Cisco OpenDNS (AS36692)	US
Panasonic (AS64294)	*Cogent Communications (AS174)	US
	**Cloudflare (AS1335) Google (AS15169)	
SITA (AS206433)	SITA (AS206433)	NL
ViaSat (AS40306)	ViaSat (AS7155)	US

* December 2023 - February 2024

** March 2025

Table 4: DNS Providers and resolver locations for GEO SNOs captured in our in-flight dataset

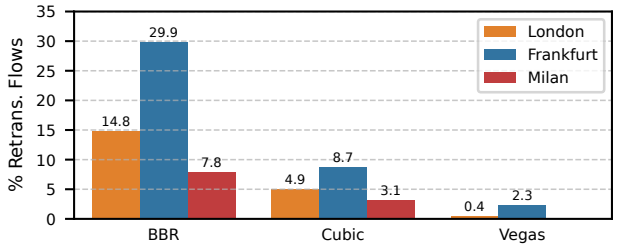

Figure 10: % of retransmissions flows by location and CCA

(for example, powered off). Finally, we also indicate the total number of tests conducted during connection to each PoP per flight.

A.6 Breakdown of TCP file transfer tests

Table 8 summarizes our setup for TCP file transfer tests, where we selected AWS server endpoints based on Starlink PoP in use. Note that Sofia lacks a nearby AWS region, and due to limited connection time in Milan, we were unable to complete Vegas evaluations.

A.7 Retransmission Rates per TCP CCA

BBR's higher can be attributed its aggressive window management strategy, which directly estimates bandwidth and RTT to model network capacity, making it resilient to random packet losses and variable latencies that challenge loss-based (Cubic) and delay-based (Vegas) CCAs in satellite networks. However, our results also highlight potential tradeoffs prompted by BBR's high bandwidth utilization. We analyze retransmission by computing *retransmission flow %*, or the proportion of 100 ms intervals containing retransmitted packets in pcap captures. Figure 10 compares the retransmission flow of CCAs for tests conducted in geographically aligned server-PoP pairs. BBR exhibits significantly higher retransmission rates than its counterparts; 3-34.3× higher in London, 3.4-12.8× in Frankfurt (peaking at 29.8%), and 2.5× in Milan. These elevated retransmissions suggest that BBR tends to overestimate available capacity in Starlink networks, causing buffer overflow and subsequent packet loss [28]. align with findings from [28] that BBR tends to overestimate available capacity in Starlink networks, causing buffer overflow and subsequent packet loss that requires retransmission.

Test	Description	Visibility	Frequency	Amigo	Amigo with Starlink Ext.
Device Status Report	Report device-level information	WiFi SSID, Public IP address, battery level, foreground application	5 minutes	Yes	Yes
Speedtest	Speedtest to an Ookla server near user's public IP address (PoP)	Latency, Up/Down Bandwidth	15 minutes	Yes	Yes
Traceroute	Traceroute to 1) `google.com` 2) `facebook.com` 3) `1.1.1.1` (Cloudflare DNS) 4) `8.8.8.8` (Google DNS)	Latency, Network Path	15 minutes	Yes	Yes
DNS Lookup	Retrieve DNS resolver from `https://nextdns.io`	DNS resolver	15 minutes	Yes	Yes
CDN	Download `jquery.min.js` (v3.6.0) from *Google CDN, Cloudflare, Microsoft Ajax, jsDelivr*, and *jQuery* via `curl`	Download speed, DNS lookup time, HTTP Headers, Cache Hit/Miss status, Edge server location	15 minutes	Yes	Yes
High-Frequency UDP	High-frequency (every 10 ms) UDP ping to AWS cloud server via `IRTT`	Latency	20 minutes (Duration: 5 minutes)	No	Yes
TCP File Transfer	Download 1800 MB file from AWS cloud server, using different TCP Congestion Control Algorithms: BBRv1, Cubic, Vegas	Download speed, socket-level statistics	20 minutes (Duration: capped at 5 minutes)	No	Yes

Table 5: Overview of tests supported by `AmiGo` and its Starlink Extension.

Airline	Origin	Destination	Departure Date	ASN/SNO	PoP Location	# Traceroutes (Google DNS)	# Traceroutes (Cloudflare DNS)	# Traceroutes (google.com)	# Traceroutes (facebook.com)	# Ookla	# CDN
AirFrance	BEY	CDG	03-01-2024	AS22351 Intelsat	Wardensville (US)	0	0	0	0	15	0
AirFrance	ATL	CDG	20-01-2024	AS64294 Panasonic	Lake Forest (US)	4	4	4	4	4	0
Emirates	DXB	ADD	22-12-2023	AS206433 SITA	Lelystad (NL)	7	7	7	6	7	35
Emirates	DXB	MEX	23-12-2023	AS206433 SITA	Lelystad (NL)	69	68	68	63	69	343
Emirates	MEX	BCN	01-01-2024	AS206433 SITA	Lelystad (NL)	5	5	5	5	5	25
Emirates	DXB	LHR	03-01-2024	AS206433 SITA	Lelystad (NL)	27	27	26	27	27	129
Emirates	KUL	DXB	02-01-2024	AS206433 SITA	Lelystad (NL)	5	5	5	5	5	25
Etihad	AUH	KUL	21-12-2023	AS64294 Panasonic	Lake Forest (US)	11	11	11	11	11	54
Etihad	ICN	AUH	07-03-2025	AS64294 Panasonic	Lake Forest (US)	23	23	23	23	22	110
Etihad	FCO	AUH	20-01-2024	AS64294 Panasonic	Lake Forest (US)	6	6	6	6	6	30
Etihad	BKK	AUH	07-01-2024	AS64294 Panasonic	Lake Forest (US)	22	22	22	22	21	0
Etihad	ICN	AUH	03-01-2024	AS64294 Panasonic	Lake Forest (US)	3	3	3	3	3	10
Etihad	AUH	ICN	14-12-2023	AS64294 Panasonic	Lake Forest (US)	24	24	24	24	24	114
Etihad	CDG	AUH	21-01-2024	AS64294 Panasonic	Lake Forest (US)	7	7	7	6	4	18
JetBlue	MIA	KIN	23-12-2023	AS40306 ViaSat	Englewood (US)	2	2	2	0	2	10
KLM	ACC	AMS	02-01-2024	AS22351 Intelsat	Wardensville (US)	0	0	0	0	11	40
Qatar	DOH	MAD	03-11-2024	AS31515 INMARSAT	Staines (GB) Greenwich (US)	23	22	10	14	23	118
Qatar	DOH	LAX	08-12-2024	AS206433 SITA	Amsterdam (NL)	9	7	7	7	5	11
SaudiA	DXB	RUH	18-02-2024	AS206433 SITA	Lelystad (NL)	1	0	1	1	0	2

Table 6: Detail of GEO-based flights in our dataset. The origin and destination airports are indicated by IATA codes.

Origin	Destination	Departure Date	PoPs	Duration (minutes)	# Traceroutes (Google DNS)	# Traceroutes (Cloudflare DNS)	# Traceroutes (google.com)	# Traceroutes (facebook.com)	# Ookla	# CDN
DOH	JFK	08-03-2025	Doha (dohaqat1)	74	6	12	6	5	6	30
			Sofia (sfiabgr1)	196	8	8	5	5	5	20
			Warsaw (wrswpol1)	20	2	2	1	1	1	5
			Frankfurt (frntdeu1)	46	6	6	4	3	3	20
			London (lndngbr1)	170	12	12	24	6	7	60
			New York (nwyynyx1)	184	13	26	13	13	13	65
JFK	DOH	16-03-2025	New York (nwyynyx1)	167	9	18	9	9	2	45
			Madrid (mdrdesp1)	55	7	8	4	3	4	20
			Milan (mlnnita1)	22	4	3	2	2	2	10
			Sofia (sfiabgr1)	172	3	6	3	1	1	15
			Doha (dohaqat1)	101	6	9	7	6	6	33
DOH	JFK	21-03-2025	Doha (dohaqat1)	73	0	0	0	0	0	0
			Sofia (sfiabgr1)	189	1	2	1	1	1	5
			Milan (mlnnita1)	54	4	4	2	2	2	10
			Madrid (mdrdesp1)	45	2	4	1	1	1	5
			London (lndngbr1)	181	3	6	3	1	3	15
			New York (nwyynyx1)	259	4	4	4	4	4	19
JFK	DOH	07-04-2025	New York (nwyynyx1)	256	2	3	2	2	1	10
			London (lndngbr1)	143	3	3	3	3	2	10
			Frankfurt (frntdeu1)	65	2	2	2	2	2	10
			Milan (mlnnita1)	46	1	1	1	1	1	5
			Sofia (sfiabgr1)	198	6	6	6	6	5	30
			Doha (dohaqat1)	71	2	2	2	2	2	10
DOH	LHR	11-04-2025	Doha (dohaqat1)	79	2	3	2	2	0	0
			Sofia (sfiabgr1)	234	9	7	6	6	3	30
			Warsaw (wrswpol1)	15	0	0	0	0	0	0
			Frankfurt (frntdeu1)	64	0	0	0	0	0	0
			London (lndngbr1)	23	0	0	0	0	0	0
LHR	DOH	13-04-2025	London (lndngbr1)	89	0	0	0	0	0	0
			Frankfurt (frntdeu1)	53	0	0	0	0	0	0
			Milan (mlnnita1)	22	0	0	0	0	0	0
			Sofia (sfiabgr1)	175	19	19	11	11	9	55
			Doha (dohaqat1)	88	2	3	2	2	2	10

Table 7: Detail of all Starlink flights in our dataset.

PoP	BBR	Cubic	Vegas
London	London	London	London
Frankfurt	London, Frankfurt	London, Frankfurt	Frankfurt
Milan	Milan	Milan	
Sofia	London		

Table 8: Breakdown of TCP CCA experiments conducted at each PoP, with AWS endpoints colored in orange.